On Burgers-Type Equations with Nonmonotonic Dissipative Fluxes

ALEXANDER KURGANOV

DORON LEVY

AND

PHILIP ROSENAU

Tel-Aviv University

Abstract

We study a formation of patterns in Burgers-type equations endowed with a bounded but nonmonotonic dissipative flux: $u_t + f(u)_x = \pm\nu Q(u_x)_x$, $Q(s) = s/(1+s^2)$. Issues of uniqueness, existence, and smoothness of a solution are addressed. Asymptotic regions of a solution are discussed; in particular, classical and nonclassical traveling waves with an embedded subshock are constructed. © 1998 John Wiley & Sons, Inc.

1 Introduction

Though the model equation proposed by Johannes Burgers in 1948 to describe turbulent flow,

$$u_t + uu_x = \nu u_{xx}\,, \tag{1.1}$$

turned out to be unsuitable for that purpose, it has became the prototypical equation for describing convective-dissipative interactions in fluids. The importance of this so-called Burgers equation for over half a century stems from its being linearizable via the Hopf-Cole map, the impetus it provided to seek similar miracles elsewhere, and its ubiquity; equation (1.1) was shown to emerge asymptotically (in the limit of small gradients and amplitudes) in a wide variety of physical settings.

While mathematical accessibility of a model is almost guaranteed to assure its popularity, very often it also fixates its position in our mind far beyond its scientific feasibility. After all, a model equation like (1.1) is only a one-dimensional toy. Its scientific (as opposed to mathematical) relevance is limited to a weakly nonlinear regime with other degrees of freedom in a problem being frozen. When a good toy model is introduced to explore new concepts, a new paradigm is born, but an untamed use may turn a good deed into scientific stagnation. It is a dangerous affair to seek in a toy what cannot be found there.

Communications on Pure and Applied Mathematics, Vol. LI, 0443–0473 (1998)
© 1998 John Wiley & Sons, Inc. CCC 0010–3640/98/050443-31

The model problem presented here is a new mathematical toy problem intended to advance our understanding of the impact that a genuinely nonlinear, saturating diffusion has on the formation of patterns in the simplest, nontrivial setup as afforded by a generalized Burgers-type model

$$u_t + f(u)_x = \nu \Big[Q(u_x) \Big]_x = \pm\nu \frac{1-u_x^2}{(1+u_x^2)^2} u_{xx} \tag{1.2}$$

where $Q(u_x) = \pm u_x/(1+u_x^2)$.

Within this very simple setting, we aim to understand certain strongly nonlinear processes that govern high amplitude/gradients phenomena where critical changes in dynamics may take place. We stress that in general we lack the tools needed for a methodical approach to such problems. Models of such processes are proposed on the basis of physical intuition and other "ingenious" means but not through a systematic derivation. Such models are not necessarily of lesser value but can only a posteriori be evaluated for their scientific merit. Genuinely nonlinear phenomena like critical transitions are, as a rule, beyond the reach of weakly nonlinear theories. Unlike the weakly nonlinear regime, it is unrealistic to expect that at large amplitudes and/or gradients only one property will evolve while the other will remain frozen (say, thermal changes that will not induce motion in a liquid or deformation in solids). Therefore the simple model we are proposing is intended only as a first step towards a better understanding of the mathematical and physical issues involved.

A degenerate version of (1.2) without the convective flux $f(u)_x$ and with a positive sign on the RHS was introduced in [10] and [9].

In our previous work [4], the dissipation flux function $Q(u_x) = u_x/(1+u_x^2)^{1/2}$ was assumed to be a monotone function in gradients. Here we go into a more evolved physical setup where not only is the dissipative flux bounded but nonmonotonic relations between gradients and the dissipation flux are assumed. The particular choice of $Q(u_x)$ in (1.2) is not a replica of a particular response; rather it is intended to be a simple caricature of complex scenarios where at a critical stress the medium yields (say, elastoplastic transit) or undergoes some critical transition accompanied by a structural change (say, a non-Newtonian behavior in complex liquids) of its characteristics and, as a consequence, its dynamical response changes drastically. While the change of sign in the elliptic part has an important impact on the dynamics, the flux saturation is at least as important in shaping the overall dynamics. Therefore, the observed phenomena in this problem are completely different from those observed in other problems where the sign of the elliptic part changes but there is no saturation of the dis-

sipative flux (see, e.g., [6, 12]). The saturation of the dissipation flux manifests itself in many ways. In linear problems the change in sign of the elliptic part would immediately trigger ill-posedness. As we shall see, the nonlinearity due to saturation mitigates this effect into a useful instability that induces formation of a global pattern.

The paper is organized as follows: In Section 2 we consider the long-wavelength variant (1.2+) without the convective term $f(u)_x$ augmented with Dirichlet boundary conditions. Our main results are captured by Theorem 2.2, which states that if the initial derivative is sufficiently small, then the solution to the Dirichlet problem tends to its corresponding steady-state solution.

In Section 3 we append the purely diffusive problem with a nonlinear convective term $f(u)_x$. First, in Section 3.1 we derive for the corresponding Cauchy problem a $W^1(L^\infty)$ a priori estimate. This estimate is then utilized in Theorem 3.2 to obtain the existence of a classical solution to the Cauchy problem as well as its uniqueness (for sufficiently small initial data). In Section 3.2 we discuss the weak limit as $\nu \downarrow 0$.

In Section 3.3 we analyze its traveling-wave solutions and demonstrate an existence of a critical threshold above which no continuous upstream-downstream trajectory is possible. We construct a supercritical solution with an embedded subshock. A proof of this fact is left to [2]. The "catastrophe" in gradients is intuitively obvious; our model imposes an upper bound on the amount of the diffusive flux while the convective flux may be as large as desired. When the fluxes are no longer in balance, smooth upstream-downstream transit becomes impossible and subshock forms. The presented numerical simulations clearly demonstrate that the constructed traveling-wave solutions are strong attractors. In Section 3.4 we characterize the asymptotic behavior of the solution to the Dirichlet problem in terms of its steady-state solution.

In Sections 4 and 5 we study the short-wavelength variant, (1.2–). The innocuous change of sign from (1.2+) creates deep qualitative changes in the resulting dynamics. In the absence of convection, our main result in Section 4 for (1.2–) is a $W^1(L^\infty)$ estimate that we derive in two independent ways: by using a formal maximum principle on the derivative and by employing L^p-iterations. In Section 5 we revisit (1.2–) appended with convection. Corollary 5.2 states a weak maximum principle that allows the L^∞-norm of the solution to (1.2–) to increase linearly with time. We present a number of numerical examples that illustrate a formation of patterns in equation (1.2–).

We stress that the purpose of the numerical examples goes beyond illustration. They are an important tool towards the unfolding of phenomena that are at this point beyond the reach of our analysis. Therefore, those exam-

ples will play a key role in future efforts to understand these genuinely non linear problems.

2 Long-Wavelength Equation: Part I

We consider first the following initial boundary value problem (IBVP):

$$u_t = \nu Q(u_x)_x\,, \quad Q(u_x) = \frac{u_x}{1+u_x^2}\,,\ t \geq 0\,,\ x \in [x_0, x_1]\,,\ \nu > 0\,, \tag{2.1}$$

augmented with the initial boundary value conditions

$$\begin{cases} u(x_0,t) = u^0, \quad u(x_1,t) = u^1, \\ u(x, t=0) = u_0(x)\,. \end{cases} \tag{2.2}$$

Rewriting equation (2.1) as

$$u_t = \nu \frac{1-u_x^2}{(1+u_x^2)^2} u_{xx} \tag{2.3}$$

makes it clear that it is stable for small gradients. However, for $|u_x| > 1$, it is unstable. As the gradients increase, the coefficient of u_{xx} in (2.3) is of the order of $1/u_x^2$, and therefore its overall influence diminishes. The following lemma characterizes the possible growth in the gradients when the initial data are sufficiently small.

LEMMA 2.1 *Consider the initial boundary value problem* (2.1)–(2.2)*. Assume that* $u_0 \in C^3[x_0, x_1]$ *and that* $\|u_0'\|_{L^\infty} < 1$*. Then* $\forall t > 0$*, the following a priori estimate holds*:

$$\|u_x\|_{L^\infty} \leq \|u_0'\|_{L^\infty}\,. \tag{2.4}$$

PROOF: Differentiating (2.1) with respect to x and denoting u_x by w, we have

$$w_t = \nu \left[\frac{1-w^2}{(1+w^2)^2}\right]_x w_x + \nu \frac{1-w^2}{(1+w^2)^2} w_{xx}\,. \tag{2.5}$$

Since $\|u_0'\|_{L^\infty} < 1$, equation (2.5) remains parabolic $\forall t > 0$, and the result follows from the familiar maximum principle. ∎

In other words, Lemma 2.1 assures that you do not enter the unstable domain if you were not initially there.

Remark. Under the assumptions of Lemma 2.1, it is possible to prove by standard arguments the existence and uniqueness of a classical solution to problem (2.1)–(2.2) (for details, consult [5]).

We now turn to the asymptotic behavior of the solutions to (2.1)–(2.2). We prove that for sufficiently small initial data, these solutions tend to the solutions of the corresponding steady-state problem. To this end we note that the unique classical solution of the steady-state problem,

$$\begin{cases} Q(v_x)_x = 0\,, \\ v(x_0,t) = u^0\,, \quad v(x_1,t) = u^1\,, \end{cases} \tag{2.6}$$

is given via

$$v(x) = \left(\frac{u_1 - u_0}{x_1 - x_0}\right)(x - x_0) + u_0\,. \tag{2.7}$$

THEOREM 2.2 (Asymptotic Steady-State Behavior) *Assume that $u(x,t)$ is a classical solution of* (2.1)–(2.2)*, that $u_0 \in C^3[x_0, x_1]$, and that $v(x)$ is a solution of* (2.6)*. If the initial derivative u_0' is sufficiently small, i.e., there exists a constant $\beta < \frac{1}{k}$, $k = |(u_1 - u_0)/(x_1 - x_0)|$, such that*

$$\|u_0'\|_{L^\infty} < \min(1, \beta), \tag{2.8}$$

then there exists a positive constant $C > 0$ such that

$$\|u(\cdot,t) - v(\cdot)\|_{L^2}^2 \le e^{-Ct}\|u_0(\cdot) - v(\cdot)\|_{L^2}^2\,. \tag{2.9}$$

COROLLARY 2.3 *Estimate* (2.9) *clearly implies that for $t \to \infty$,*

$$\|u(\cdot,t) - v(\cdot)\|_{L^2} \to 0\,. \tag{2.10}$$

PROOF: Let w be the difference between the solutions of (2.1)–(2.2) and (2.6), i.e., $w(x,t) = u(x,t) - v(x)$. We multiply (2.1) and (2.6) by a test function $\varphi \in C_0^1$ and integrate by parts to obtain

$$\int_{x_0}^{x_1} w_t\varphi\,dx + \nu\int_{x_0}^{x_1}\left[\left(\frac{u_x}{1+u_x^2}\right) - \left(\frac{v_x}{1+v_x^2}\right)\right]\varphi_x\,dx = 0\,. \tag{2.11}$$

In particular, for the choice $\varphi = w$ in (2.11), we obtain (since $v_x = \pm k$)

$$\frac{1}{2}\frac{d}{dt}\|w(\cdot,t)\|_{L^2}^2 + \frac{\nu}{1+k^2}\int_{x_0}^{x_1}\frac{1 \pm ku_x}{(1+u_x^2)}w_x^2\,dx = 0\,. \tag{2.12}$$

According to assumption (2.8) we have

$$\|1 \pm k u_x\|_{L^\infty} \geq 1 - k\beta\,.$$

On the other hand, due to the same assumption, Lemma 2.1 provides

$$\frac{1}{1+u_x^2} \geq \frac{1}{1+\|u_0'\|_{L^\infty}^2} \geq \frac{1}{2}\,.$$

Consequently, (2.12) becomes

$$\frac{d}{dt}\|w(\cdot,t)\|_{L^2}^2 + C_1\|w_x(\cdot,t)\|_{L^2}^2 \leq 0\,, \tag{2.13}$$

where $C_1 = \nu\frac{1-k\beta}{1+k^2} > 0$. Applying Friedrichs inequality [1] and Gronwall's lemma [3] on inequality (2.13) produces the desired estimate (2.9) with the promised constant $C = C_1(x_1 - x_0)$. ∎

It behooves us at this point to present two numerical examples of solutions to the IBVP (2.1)–(2.2). Neither example falls under the scope of Theorem 2.2: In the first example, the initial datum is smooth but large; in the second example, the initial datum is a discontinuous step function. In both cases, the numerical solution tends to the corresponding steady-state solution. Such behavior is guaranteed by Theorem 2.2 for small initial data but appears to hold independently of this constraint.

In both examples, we solved the IBVP (2.1)–(2.2) for $x \in [x_0, x_1] = [-1, 1]$, $t \geq 0$, $\nu = 1$. The Dirichlet boundary conditions were set such that for $u(x,0) = u_0(x)$,

$$u^0 = u_0(x_0)\,, \qquad u^1 = u_0(x_1)\,. \tag{2.14}$$

In the first problem we used a Gaussian initial datum

$$u_0(x) = e^{-40x^2}\,, \quad x \in [-1, 1]\,. \tag{2.15}$$

The results are plotted in Figure 2.1.

The second example corresponds to the discontinuous initial datum

$$u_0(x) = \begin{cases} 1\,, & -1 \leq x < 0\,, \\ 0\,, & 0 < x \leq 1\,. \end{cases} \tag{2.16}$$

In Figure 2.2 the numerical results are displayed. As expected, at large times the solution converges to the straight line connecting the boundary points.

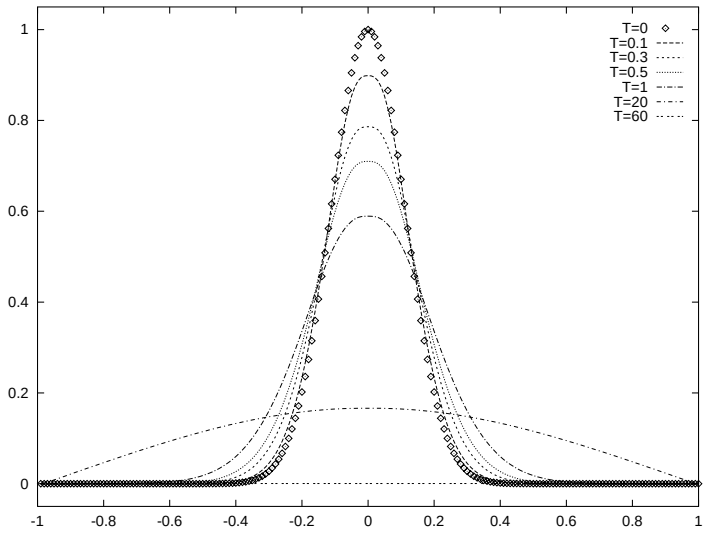

Figure 2.1. Gaussian initial data for problem (2.1)/(2.15).

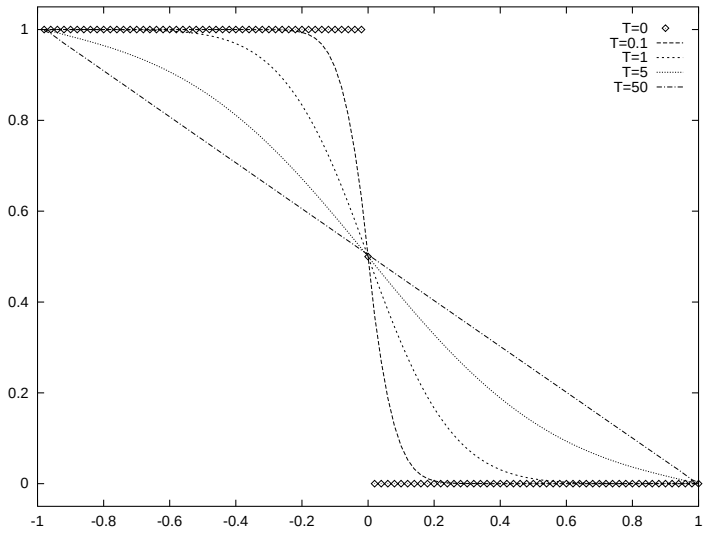

Figure 2.2. Discontinuous initial data for problem (2.1)/(2.16).

3 Long-Wavelength Equation: Part II

We now append to equation (2.1) a smooth, nonlinear *convective flux function* $f(u)_x$ to recover the full equation (1.2+). Explicitly,

$$u_t + f(u)_x = \nu Q(u_x)_x\,, \quad Q(u_x) = \frac{u_x}{1+u_x^2}\,,\ t \geq 0\,,\ \nu > 0\,, \tag{3.1}$$

which may thus be seen to be an extension of the Burgers equation. The RHS of (3.1) remains the same as in (2.1) and hence is stable only for $|u_x| < 1$.

3.1 Existence and Uniqueness of Classical Solutions

Consider the Cauchy problem for (3.1) augmented with periodical or compactly supported initial data

$$u(x, t{=}0) = u_0(x)\,. \tag{3.2}$$

We begin with an L^∞-bound on the derivative for a sufficiently small initial datum, as guaranteed by the following:

LEMMA 3.1 ($W^1(L^\infty)$ A Priori Estimate) *Let $u(x,t)$ be a classical solution of problem* (3.1)–(3.2)*. If*

$$\nu \left\| \frac{u_0'}{1+(u_0')^2} \right\|_{L^\infty} + 2\|f(u_0)\|_{L^\infty} \leq \alpha < \frac{\nu}{2}\,, \quad \|u_0'\|_{L^\infty} < 1\,, \tag{3.3}$$

then $\forall t \geq 0$,

$$\|u_x(\cdot,t)\|_{L^\infty} \leq C\,. \tag{3.4}$$

PROOF: Following [4, sec. 5] one can derive (utilizing the maximum principle on u), the following estimate:

$$\nu \left| \frac{u_x(x,t)}{1+u_x^2(x,t)} \right| \leq \nu \left\| \frac{u_0'}{1+(u_0')^2} \right\|_{L^\infty} + 2\,\|f(u_0)\|_{L^\infty}\,, \quad t \geq 0\,. \tag{3.5}$$

The RHS of (3.5) is bounded due to assumption (3.3). Hence, for a sufficiently small initial datum (3.3),

$$\nu \left| \frac{u_x(x,t)}{1+u_x^2(x,t)} \right| \leq \alpha\,, \tag{3.6}$$

and in spite of the nonmonotonic behavior of $Q(u_x)$, u_x remains bounded (consult Figure 3.1). ∎

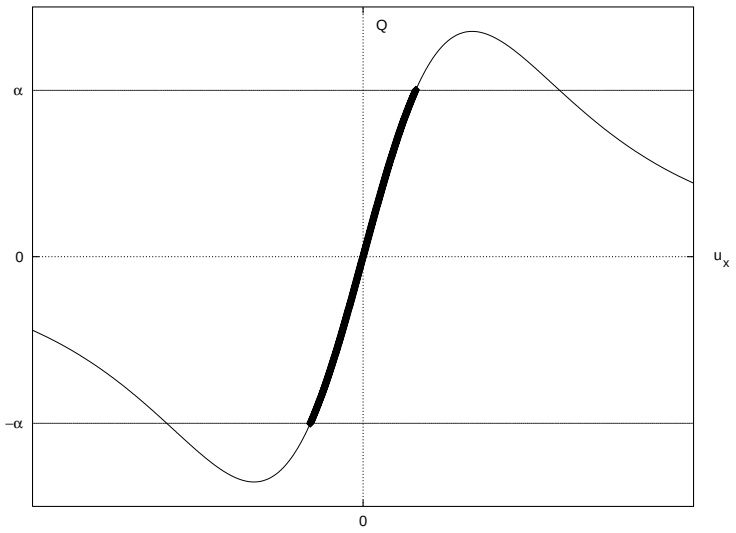

Figure 3.1. $Q(u_x)$.

Following the arguments presented in [4, secs. 3 and 5], it is also possible to prove the existence and uniqueness of a classical solution to (3.1)–(3.2) by the vanishing-viscosity method. To this end, we consider

$$\begin{cases} u_t^\delta + f(u^\delta)_x = \nu \left(\frac{u_x^\delta}{1+(u_x^\delta)^2} \right)_x + \delta u_{xx}^\delta \\ u^\delta(x,0) = u_0(x) \end{cases} \qquad \delta > 0\,. \tag{3.7}$$

The smooth solution of the viscous problem (3.7) depends on the (small) parameter δ. Utilizing Lemma 3.1 and following similar arguments to those found in [4], the existence and uniqueness of a solution of (3.1)–(3.2) can be shown by taking the limit $\delta \downarrow 0$. We summarize these results in the following:

THEOREM 3.2 (Existence and Uniqueness) *Consider the problem* (3.1)–(3.2). *Assume that the initial datum* $u_0(x) \in C^3$ *satisfies* (3.3). *Then there exists a unique global classical solution* $u(x,t) \in C^{2,1}(x,t)$.

3.2 Convergence as $\nu \downarrow 0$

We analyze the behavior of solutions of equation (3.1) as the parameter ν tends to zero. To clarify the dependence of the solution on ν, we rewrite (3.1) as

$$u_t^\nu + f(u^\nu)_x = \nu \Big[Q(u_x^\nu) \Big]_x\,, \quad Q(u_x^\nu) = \frac{u_x^\nu}{1+(u_x^\nu)^2}\,,\ \nu > 0\,. \tag{3.8}$$

Since $Q(u_x^\nu)$ is bounded, it is possible to overcome the difficulty due to the u_x terms and formally define weak solutions of (3.8) [11]. Even though existence and uniqueness results of such weak solutions are currently unavailable, we have the following:

THEOREM 3.3 (Convergence Rate) *Assume that u^ν is a solution of* (3.8) *subject to L^∞-bounded initial conditions $u^\nu(x,0) \equiv u_0(x)$. Then u^ν converges to the unique entropy solution of*

$$u_t + f(u)_x = 0$$

as $\nu \downarrow 0$, and the following error estimates hold for all $t \geq 0$:

$$\|u^\nu(\cdot,t) - u(\cdot,t)\|_{W^{-1}(L^\infty)} \leq \text{const}_t \cdot \nu\,, \tag{3.9}$$

$$\|u^\nu(\cdot,t) - u(\cdot,t)\|_{L^p} \leq \text{const}_t \cdot \nu^{1/p}\,, \qquad 2 \leq p \leq \infty\,, \tag{3.10}$$

$$\|u^\nu(\cdot,t) - u(\cdot,t)\|_{L^1} \leq \text{const}_t \cdot \sqrt{\nu}\,. \tag{3.11}$$

The proof of Theorem 3.3 is based on the boundedness of Q and is analogous to the proof of theorem 4.1 in [4] due to [13, prop. 2.1].

3.3 Traveling Waves

We consider the traveling-wave solutions for equation (3.1). Throughout this section we let $\nu = 1$, $f(u) = u^2/2$, and choose $u = 0$ and $u = u_1$ to be the upstream and downstream values, respectively. Let $z = x - \lambda t$; then one integration of (3.1) yields

$$-\lambda u + \frac{u^2}{2} = \frac{u_z}{1+u_z^2} + C\,, \quad C = \text{const}\,. \tag{3.12}$$

The derivative u_z has to vanish for $u = 0$ and $u = u_1$, and hence $C = 0$ and the downstream amplitude is related to the wave speed via $u_1 = 2\lambda$. Solving (3.12) with respect to u_z yields

$$u_z = \frac{1 \pm \sqrt{1 - u^2(u-u_1)^2}}{u(u-u_1)}\,. \tag{3.13}$$

Clearly, a continuous trajectory connecting the upstream and downstream exists provided that the discriminant is not negative. The critical transition occurs at $u_1 = 2$ ($\lambda = 1$). Above this critical value, only a discontinuous upstream-downstream transit is possible. Such a discontinuity must be connected by a subshock. The size of the jump across the subshock can easily be found to be

$$[u] = \sqrt{u_1^2 - 4}\,. \tag{3.14}$$

The results obtained so far in this section are formal. We can prove, though, that under suitable conditions on Q, "catastrophe in gradients" always occurs, as finite gradients become infinite within a finite time. The proof of this fact will be detailed in [2].

At this point we present a number of numerical experiments intended to demonstrate that these traveling-wave solutions are attractors. In our examples, we imposed a symmetric upstream-downstream profile with $u_{\text{left}} = -u_{\text{right}}$, so that the resulting wave is stationary. In this case, the jump across the subshock becomes

$$[u] = 2\sqrt{u_{\text{left}}^2 - 1}\,.$$

In all of the numerical examples in this section, the boundaries were held at the constant values (2.14). Since the interval is large, the boundaries have no influence and the numerics can be considered as the solution of the problems on an infinite domain. In the first example, the initial datum is taken as

$$u_0(x) = -\frac{\sqrt{5}}{10}\tanh(x)\,, \quad x \in [-50, 50]\,. \tag{3.15}$$

The results obtained are shown in Figure 3.2.

The second example, shown in Figure 3.3, describes the numerical convergence of a discontinuous, subcritical initial datum

$$u_0(x) = \begin{cases} \frac{\sqrt{5}}{10}\,, & x < 0\,, \\ -\frac{\sqrt{5}}{10}\,, & 0 < x\,, \end{cases} \tag{3.16}$$

(which corresponds to a Riemann problem) to the smooth attractor.

In Figures 3.4 and 3.5, supercritical initial states are shown. In Figure 3.4 the initial datum is smooth, while Figure 3.5 shows the results obtained with a discontinuous Riemann datum. In these examples, $u_{\text{left}} = \sqrt{5}$.

We recall that in order to carry out these numerical experiments, the values at the boundaries were kept at a constant value. Thus, de facto we solved a Dirichlet problem. In the next section we directly address a subcritical variant of the Dirichlet problem.

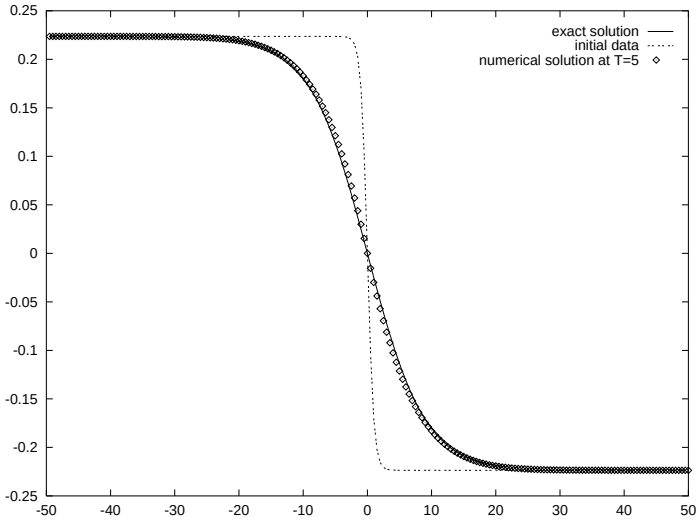

Figure 3.2. Subcritical state for initial datum (3.15).

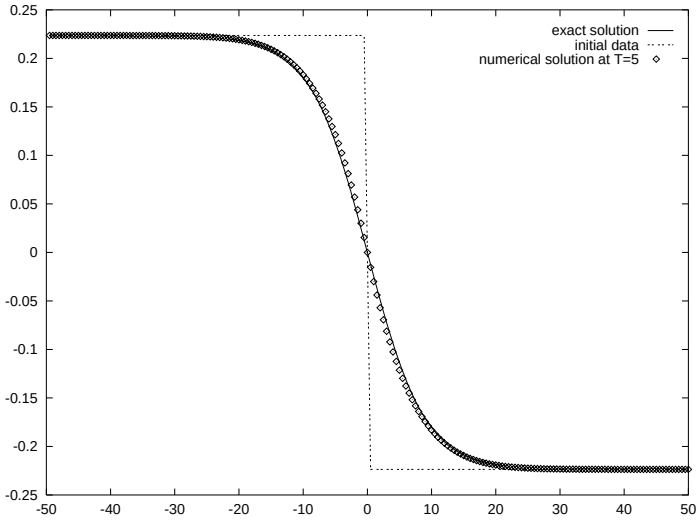

Figure 3.3. Subcritical state for the Riemann problem.

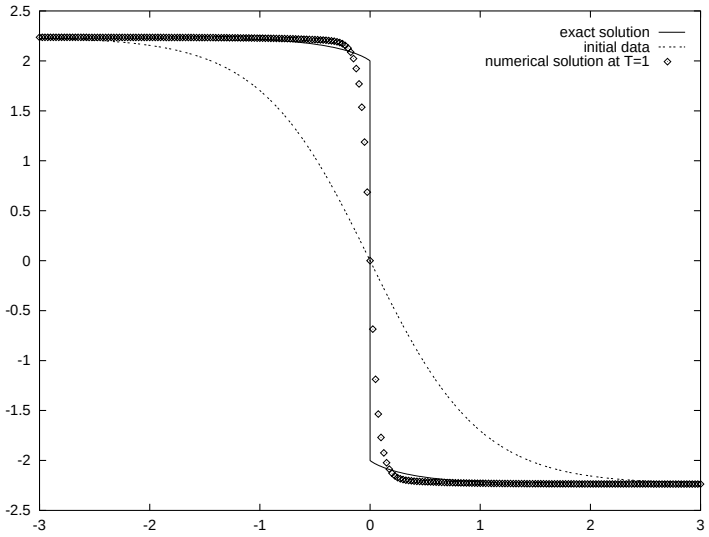

Figure 3.4. Supercritical state for $\tanh$ initial data.

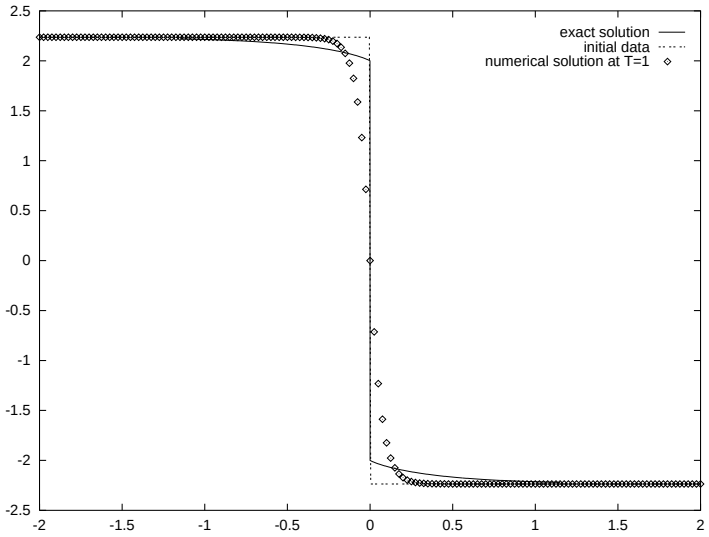

Figure 3.5. Supercritical state for the Riemann problem.

3.4 Dirichlet Problem

We consider the asymptotic behavior of solutions of (3.1) augmented with

$$\begin{cases} u(x_0,t) = u(x_1,t) = u^0\,, \\ u(x,t=0) = u_0(x)\,. \end{cases} \tag{3.17}$$

Admittedly, the assumption on the boundary values is quite restrictive because it eliminates patterns of the type shown in the last section. On the other hand, in the case studied here we can present a systematic analysis.

Our main result states that as $t \to \infty$, the solution of (3.1)/(3.17) tends to the solution of the corresponding steady-state problem

$$\begin{cases} f(v)_x = \nu\Big(\frac{v_x}{1+v_x^2}\Big)_x, \\ v(x_0,t) = v(x_1,t) = u^0\,. \end{cases} \tag{3.18}$$

The constant $v(x) \equiv u^0$ is the trivial classical solution of the steady-state problem (3.18).

ASSERTION 3.4 *Consider the problem* (3.18)*. If we require the additional relation between the fluxes at the boundaries*

$$\left(\frac{vv_x}{1+v_x^2}\right)\Big|_{x=x_1} \le \left(\frac{vv_x}{1+v_x^2}\right)\Big|_{x=x_0}, \tag{3.19}$$

then the problem admits a unique classical solution, which is the constant $v(x) \equiv u^0$.

PROOF: Multiplying (3.18) by v and integrating over the interval $[x_0, x_1]$ results in

$$\int_{x_0}^{x_1} v f(v)_x\,dx = \nu \int_{x_0}^{x_1} \left(\frac{v_x}{1+v_x^2}\right)_x v\,dx\,. \tag{3.20}$$

After an integration by parts, the LHS of (3.20) vanishes, while its RHS is

$$-\nu \int_{x_0}^{x_1} \frac{v_x^2}{1+v_x^2}\,dx + \nu \left(\frac{vv_x}{1+v_x^2}\right)\Big|_{x_0}^{x_1},$$

and due to assumption (3.19), it is nonpositive. Hence, as claimed, $v_x \equiv 0$. ∎

For sufficiently small initial data that satisfy (3.3), the L^2-distance between the classical solution of problem (3.1)/(3.17) and the constant steady-state solution $u(x) \equiv u^0$ tends to zero as $t \to \infty$ as stated in the following theorem:

THEOREM 3.5 (Asymptotic Behavior) *Let $u(x,t)$ be a classical solution of* (3.1)/(3.17)*, and assume that $u_0(x) \in C^3[x_0, x_1]$ and satisfies condition* (3.3)*. Then there exists a positive constant $C > 0$ such that*

$$\|u(\cdot,t) - u^0\|_{L^2}^2 \le e^{-Ct}\|u_0(\cdot) - u^0\|_{L^2}^2 \,. \tag{3.21}$$

PROOF: We denote by w the difference between the solution of (3.1) and (3.17) and u^0, i.e., $w(x,t) = u(x,t) - u^0$. Following the lines of the proof of Theorem 2.2, we obtain

$$\frac{1}{2}\frac{d}{dt}\|w(\cdot,t)\|_{L^2}^2 + \int_{x_0}^{x_1} f(u)_x w \, dx + \nu \int_{x_0}^{x_1} \frac{1}{1+u_x^2} w_x^2 \, dx = 0 \,. \tag{3.22}$$

Since integration by parts yields

$$\int_{x_0}^{x_1} f(u)_x w \, dx = -\int_{x_0}^{x_1} f(u) u_x \, dx = 0 \,,$$

the second term in (3.22) vanishes.

Lemma 3.1 provides an upper bound on $\|u_x\|_{L^\infty}$. Hence, $(1 + u_x^2)^{-1}$ is bounded away from zero, and we conclude by proceeding analogously to the proof of Theorem 2.2. ∎

Note that Theorem 3.5 does not contradict the numerical examples presented in the previous section, where the boundaries are held at different values of u.

Let us illustrate the asymptotic behavior of solutions of (3.1)/(3.17) with a numerical example; the assumed initial datum is

$$u_0(x) = 2\sin(2\pi x) \,, \quad x \in [-1, 1] \,, \tag{3.23}$$

and the boundaries are held at the fixed values (3.17).

The results are plotted in Figure 3.6. As expected, convection causes the profile to sharpen. It looks as if a shock has formed, though this was not explicitly stated in our results. Eventually the pattern evolves towards the trivial steady-state solution.

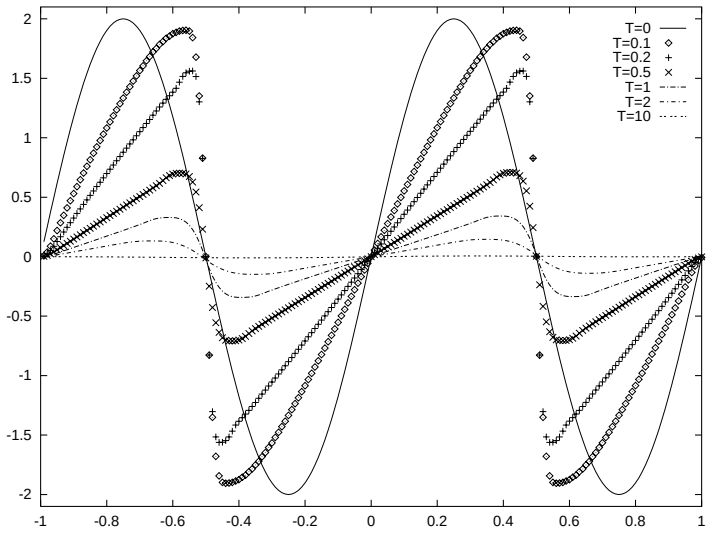

Figure 3.6. Sinusoidal initial data for problem (3.1)/(3.23).

Remarks.

1. Since the initial datum in this example is not small, it does not fall into the scope of Theorem 3.5. Nevertheless, in this numerical example and many others, the numerical solution appears to converge to the corresponding steady state. This indicates that the limitation to a small initial datum, as imposed by Theorem 3.5, is only a technical one.

2. The numerical examples presented in Section 2 were computed using a centered, second-order Lax-Friedrichs-type scheme. The numerical examples in Section 3 were computed using a central, second-order Nessyahu-Tadmor scheme [7], which was originally developed in the context of numerical solutions for hyperbolic conservation laws and was therefore able to capture the expected shocks. A systematic stability and convergence analysis of numerical schemes for the present problems is a highly nontrivial affair and is left to a future work.

4 Short-Wavelength Equation: Part I

The change of sign in (1.2+) that begets the short-wave equation (1.2–) introduces deep qualitative changes in the resulting dynamics. We start with the

nonconvective case

$$u_t = \nu Q(u_x)_x\,, \quad Q(u_x) = -\frac{u_x}{1+u_x^2},\ t \geq 0\,,\ \nu > 0\,, \tag{4.1}$$

augmented with the initial datum

$$u(x, t{=}0) = u_0(x) \tag{4.2}$$

and homogeneous Neumann boundary conditions

$$u_x(x_0, t) = 0\,, \qquad u_x(x_1, t) = 0\,. \tag{4.3}$$

For long waves, (2.1), equation (4.1) is a backward equation. Therefore, unlike (2.1), there is no classical maximum principle for $u(x,t)$. Though the questions of existence and uniqueness of solutions to this problem are highly nontrivial, surprisingly, the following strong a priori estimates on u_x hold:

LEMMA 4.1 ($W^1(L^1)$ A Priori Estimate) *Consider the IBVP* (4.1)–(4.3)*, and assume that the initial datum* $u_0 \in W^1(L^1)$*. Then for* $t \leq T$*, its classical solution satisfies*

$$\|u_x(\cdot, t)\|_{L^1} \leq \|u_0'(\cdot)\|_{L^1} + 2(x_1 - x_0)\,. \tag{4.4}$$

PROOF: Differentiating equation (4.1) with respect to x and denoting $w = u_x$, we obtain

$$w_t = \nu Q(w)_{xx}\,. \tag{4.5}$$

Multiplying (4.5) by $\operatorname{sgn}(|w| - 1)\operatorname{sgn}(w)$ followed by an integration over (x_0, x_1) yields

$$\begin{aligned} \frac{d}{dt}\||w(\cdot,t)| - 1\|_{L^1} &= \nu \int_{x_0}^{x_1} Q(w)_{xx} \operatorname{sgn}(|w| - 1)\operatorname{sgn}(w) dx \\ &= \sum_j \zeta(\sigma_j) \frac{w^2 - 1}{(1+w^2)^2} w_x \Big|_{x^{\mathrm{l}}_{\sigma_j}}^{x^{\mathrm{r}}_{\sigma_j}}. \end{aligned} \tag{4.6}$$

Here every pair $(\sigma_j, \zeta(\sigma_j))$ is one of the following:

$$\begin{cases} \sigma = \{x \mid w(x) > 1\}\,, & \zeta(\sigma) = +1\,, \\ \sigma = \{x \mid w(x) < -1\}\,, & \zeta(\sigma) = -1\,, \\ \sigma = \{x \mid 0 < w(x) < 1\}\,, & \zeta(\sigma) = -1\,, \\ \sigma = \{x \mid -1 < w(x) < 0\}\,, & \zeta(\sigma) = +1\,, \end{cases} \tag{4.7}$$

where by $x^{\mathrm{r}}_{\sigma_j}$ and $x^{\mathrm{l}}_{\sigma_j}$ we denote the right and left edges of the interval σ_j, respectively.

It is easy to see that every addend in the sum of the RHS of (4.6) is nonpositive, and inequality (4.4) follows. ∎

The $W^1(L^1)$ estimate, (4.4), implies by standard arguments the boundedness of solutions of (4.1)–(4.3), as stated by the following:

COROLLARY 4.2 (Maximum Principle) *Consider the IBVP* (4.1)–(4.3)*, and assume that the initial datum* $u_0 \in W^1(L^1)$*. Then for* $t \leq T$*, its classical solution satisfies*

$$\|u(\cdot,t)\|_{L^\infty} \leq C\,. \tag{4.8}$$

Here the constant C *depends on the initial datum* u_0 *and on the size of the domain* $(x_1 - x_0)$.

The $W^1(L^1)$ bound, as provided by Lemma 4.1, enables us to proceed with similar a priori estimates for $W^1(L^p)$, $p \geq 2$. First, we treat the case $p = 2$.

LEMMA 4.3 ($W^1(L^2)$ A Priori Estimate) *Consider the IBVP* (4.1)–(4.3)*, and assume that the initial datum* $u_0 \in W^1(L^2)$*. Then for* $t \leq T$*, its classical solution satisfies*

$$\|u_x(\cdot,t)\|_{L^2} \leq C\,, \tag{4.9}$$

where the constant C *depends on* $\|u_0'\|_{L^2}$*,* $\|u_0'\|_{L^1}$*, and the size of the* x*-domain* $(x_1 - x_0)$.

PROOF: Multiplying (4.5) by $(w - 2\arctan w)$ and integrating over the interval (x_0, x_1) implies

$$\begin{aligned}
&\frac{d}{dt}\int_{x_0}^{x_1}\left(\frac{w^2}{2} - 2w\arctan w + \ln(1+w^2)\right)dx \\
&\quad = \nu\int_{x_0}^{x_1} Q(w)_{xx}(w - 2\arctan w)dx \\
&\quad = -\nu\int_{x_0}^{x_1}\frac{w^2-1}{(1+w^2)^2}\left(1 - \frac{2}{1+w^2}\right)w_x^2\,dx \leq 0\,,
\end{aligned}$$

which, in turn, carries

$$\int_{x_0}^{x_1}\left(\frac{w^2}{2} - 2w\arctan w + \ln(1+w^2)\right)dx \leq C_0\,,$$

where $C_0 = C_0(\|u_0'\|_{L^2}, \|u_0'\|_{L^1})$. Using Lemma 4.1 we can bound

$$2\int_{x_0}^{x_1} (w \arctan w)\, dx \le \pi \|w\|_{L^1} \le \pi \|u_0'\|_{L^1}\,,$$

and the L^2-estimate (4.9) follows. ∎

We may now turn to the general case.

LEMMA 4.4 ($W^1(L^p)$ A Priori Estimate) *Consider the IBVP* (4.1)–(4.3)*, and assume that the initial datum $u_0 \in W^1(L^p)$. Then for $t \le T$ and for even $p = 2m$, its classical solution satisfies*

$$\|u_x(\cdot, t)\|_{L^p} \le C^{1/m} + K\,, \tag{4.10}$$

where the constants C and K depend on the initial datum u_0 and on the length of the x-domain $(x_1 - x_0)$.

PROOF: We multiply (4.5) by

$$\left(\frac{w^{2m-1}}{2m-1} - \frac{w^{2m-3}}{2m-3}\right)$$

and integrate by parts to obtain

$$\frac{d}{dt}\int_{x_0}^{x_1} \left(\frac{w^{2m}}{(2m)(2m-1)} - \frac{w^{2m-2}}{(2m-2)(2m-3)}\right) dx \le 0\,.$$

Hence,

$$\begin{aligned}
\frac{d}{dt}\int_{x_0}^{x_1} w^{2m}\, dx &\le \frac{2m(2m-1)}{(2m-2)(2m-3)} \frac{d}{dt}\int_{x_0}^{x_1} w^{2m-2}\, dx \\
&\le \frac{2m(2m-1)}{(2m-4)(2m-5)} \frac{d}{dt}\int_{x_0}^{x_1} w^{2m-4}\, dx \\
&\le \cdots \le m(2m-1)\frac{d}{dt}\int_{x_0}^{x_1} w^2\, dx\,.
\end{aligned}$$

We therefore have the following estimate:

$$\begin{aligned}
&\int_{x_0}^{x_1} w^{2m}(x,t)dx \\
&\quad \le \int_{x_0}^{x_1} w^{2m}(x,0)dx + m(2m-1)\int_{x_0}^{x_1} w^2(x,t)dx \\
&\qquad - m(2m-1)\int_{x_0}^{x_1} w^2(x,0)dx\,,
\end{aligned}$$

which, in turn, yields

$$\left(\int_{x_0}^{x_1} w^{2m}(x,t)dx\right)^{1/2m} \leq \left(m(2m-1)\int_{x_0}^{x_1} w^2(x,t)dx\right)^{1/2m} + K$$

and the desired estimate (4.10) follows by Lemma 4.3. ∎

Taking the limit $p \to \infty$ in the L^p-estimate (4.10) leads to the key result of this section:

COROLLARY 4.5 ($W^1(L^\infty)$ A Priori Estimate) *Consider the IBVP* (4.1)–(4.3)*, and assume that the initial datum* $u_0 \in W^1(L^2)$*. Then for* $t \leq T$*, its classical solution satisfies*

$$\|u_x(\cdot,t)\|_{L^\infty} \leq C\,. \tag{4.11}$$

Remarks.

1. It is clear that estimates similar to (4.10) hold for all p's.
2. The $W^1(L^2)$ a priori estimate (4.9) implies that the solution of (4.1)–(4.3) remains continuous with respect to x for initial datum $u_0 \in W^1(L^2)$.
3. It is possible to derive similar results for the periodic boundary conditions
$$u(x_0) = u(x_1) \quad \text{and} \quad u_x(x_0) = u_x(x_1)\,.$$
4. Analogous results can also be obtained for the Cauchy problem with a compactly supported initial datum. In this case, the resulting bounds on the derivatives also depend on the size of the support of the solution. Hence, if the support of the solution does not increase in time or if it grows at finite speed, the derivative is bounded in the L^p-norm. We do not know if any of these conditions hold at all, but a numerical result presented below hints that such a conjecture is reasonable.

An alternative proof to the above a priori estimates can be derived as follows using a formal maximum principle on the derivative u_x:

LEMMA 4.6 ($W^1(L^\infty)$ A Priori Estimate II) *Consider the IBVP* (4.1)–(4.3)*, and assume that the initial data are smooth. Then for* $t \leq T$*, its classical solution satisfies*

$$\|u_x(\cdot,t)\|_{L^\infty} \leq \max(\|u_0'(\cdot)\|_{L^\infty}, 1)\,. \tag{4.12}$$

PROOF: Differentiating (4.1) with respect to x and denoting $w = u_x$, we obtain

$$w_t = \nu \frac{w^2 - 1}{(1 + w^2)^2} w_{xx} + \nu \left(\frac{w^2 - 1}{(1 + w^2)^2} \right)_x w_x \, .$$

For $y(t) := \max_x w(x, t)$, we deduce that either $y(t) < 1$ or $\dot{y} \leq 0$. Similar arguments hold for the minimum of w, and the lemma follows. ∎

Remark. The proof of Lemma 4.6 can also be extended to more general problems like the following:

1. For the IBVP

$$\begin{cases} u_t = \nu Q(u_x)_x \, , \quad u(x, 0) = u_0(x) \, , \\ u_x(x_0, t) = p_0(t) \, , \quad u_x(x_1, t) = p_1(t) \, , \end{cases}$$

   where $|p_0(t)| \leq P_0$, $|p_1(t)| \leq P_1$, and P_0 and P_1 are constants, the classical solution satisfies

$$\|u_x(\cdot, t)\|_{L^\infty} \leq \max(\|u_0'(\cdot)\|_{L^\infty}, 1, P_0, P_1) \, .$$

2. For the Cauchy problem with smooth initial datum

$$u_t = \nu Q(u_x)_x \, , \quad u(x, 0) = u_0(x) \, ;$$

   the classical solution satisfies the same estimate, (4.12). Note that unlike the L^p-iterations technique, the size of the support plays no role when using the formal maximum principle on u_x.

In what follows we present a number of numerical simulations of equation (4.1) ($\nu = 1$) with the same Lax-Friedrichs-type scheme implemented in Section 2.

Example 1. First we consider equation (4.1) with homogeneous Neumann boundary conditions, (4.3), and initial datum

$$u_0(x) = e^{-0.25x^2}, \quad x \in [-5, 5] \, . \tag{4.13}$$

The numerical results are plotted in Figure 4.1. The solution tends to a constant steady state, which is consistent with the conservation of u and the stability of the solution for large gradients.

Example 2. The initial datum is now

$$u_0(x) = x^6 - 3.5x^4 + 3.5x^2 - 0.6\,, \quad x \in [-1, 1]\,, \tag{4.14}$$

supplemented with nonhomogeneous Neumann boundary conditions,

$$u_x(-1, t) = 1\,, \quad u_x(1, t) = -1\,. \tag{4.15}$$

Notably, the a priori estimates presented in this section still hold with these boundary conditions.

Observe that the solution evolves in two stages. In the first stage (on a short time scale), it evolves into a piecewise-linear pattern in which all slopes equal ± 1. In a later stage, the solution grows in time but retains its shape. Note that $\partial_t \int_{-1}^{1} u(x,t)dx = 1$, and the L^2-norm of the solution increases. These trends are clearly seen in Figure 4.2.

Example 3. We use boundary conditions (4.15) and the initial datum

$$u_0(x) = 12x^4 - 24.5x^2 + 12.5\,, \quad x \in [-1, 1]\,. \tag{4.16}$$

This example, shown in Figure 4.3, demonstrates that the ultimate pattern does not depend on the size of the initial gradients. Again, the evolution follows two stages. In the first stage the solution organizes into a triangular shape with slopes equal to ± 1. At large times, the triangular shape remains, but its amplitude increases in tandem with the increase in its L^2-norm.

Example 4. See Figure 4.4. There equation (4.1) is solved using the Dirichlet boundary condition (2.14) and the initial datum

$$u_0(x) = e^{-10x^2}, \quad x \in [-1, 1]\,. \tag{4.17}$$

The solution is seen to converge upon a steady state, which is a triangle (with slopes = ± 1) formed in the center of the region.

Note that the emergence of the sharp corners in the last example agrees with our a priori estimates. Also, as expected, the regions of small gradients in Figure 4.4 are unstable. However, there is a more basic issue involved because the emerging solution is a weak one, and as such it is not unique (for instance, take any of its translations along the line). Without a selection principle, we cannot exclude infinite other possibilities. The numerics, however, seem to capture the solution centered around the local peak.

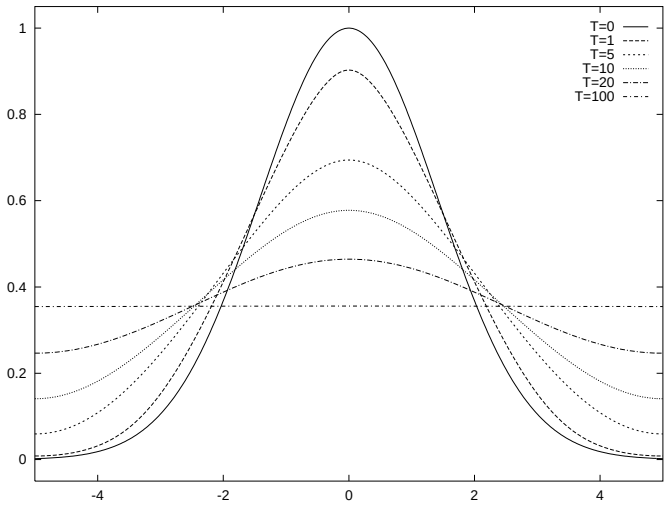

Figure 4.1. Gaussian initial data for problem (4.1)/(4.13) with homogeneous Neumann boundary values (4.3).

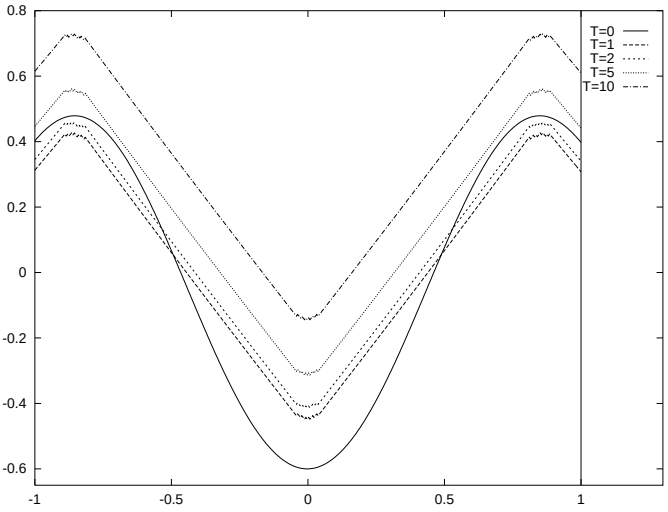

Figure 4.2. Polynomial initial data for problem (4.1)/(4.14) with nonhomogeneous Neumann boundary values (4.15); $0 \leq t \leq 10$.

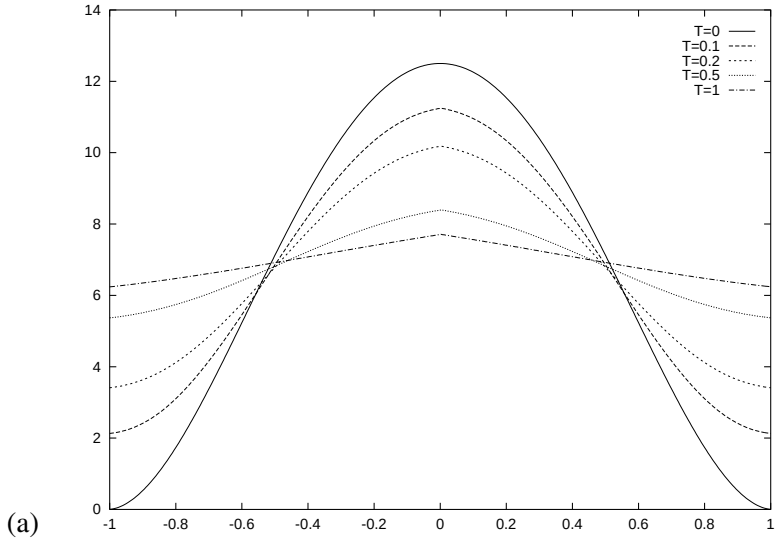

(a)

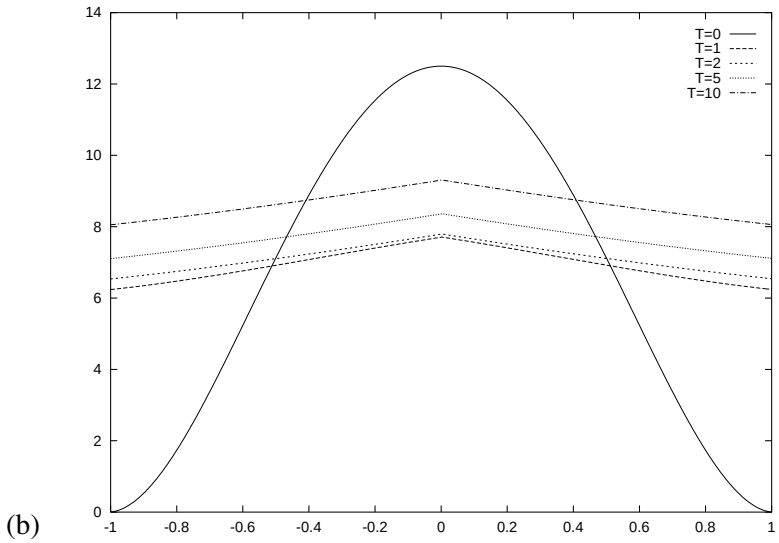

(b)

Figure 4.3. Polynomial initial data for problem (4.1)/(4.16) with nonhomogeneous Neumann boundary values (4.15). (a) $0 \leq t \leq 1$. (b) $0 \leq t \leq 10$.

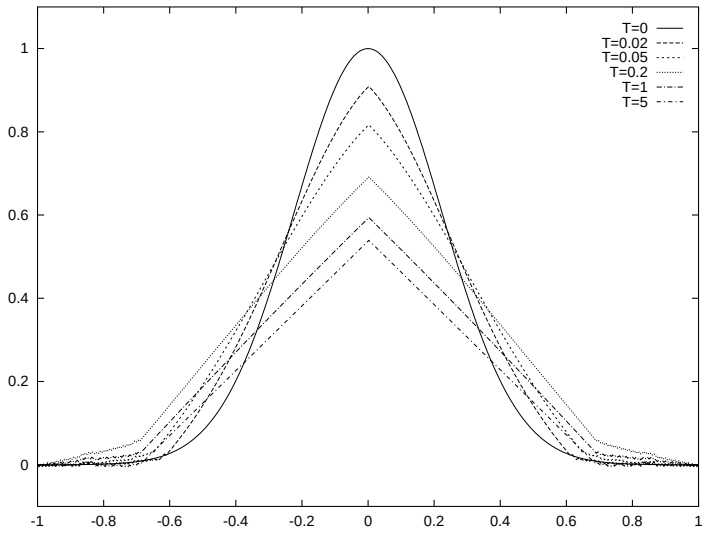

Figure 4.4. Gaussian initial data for problem (4.1)/(4.17) with Dirichlet boundary values (2.14).

5 Short-Wavelength Equation: Part II

We now append to equation (4.1) a nonlinear convection,

$$u_t + f(u)_x = \nu Q(u_x)_x\,, \quad Q(u_x) = -\frac{u_x}{1+u_x^2}\,,\ t \geq 0\,,\ \nu > 0\,. \tag{5.1}$$

As before, the convective flux $f(u)$ is assumed to be an arbitrary smooth function.

Computations analogous to those of Section 3.3 show that a traveling-wave solution for (5.1), with $f(u) = u^2/2$, exists, and it is a reflection ($z \to -z$) of the solution in (3.12). This solution, however, *cannot be stable for a convex convective flux*. Alternatively, given a concave convective flux, e.g., $f(u) = -u^2/2$, the wave traveling to the left is identical to the traveling wave in Section 3.3 and is thus stable. It is also important to note that we do not know if equation (5.1) can develop shocks during the evolution of smooth data, and numerics do not provide convincing evidence either way.

The presence of convection causes a major difficulty in obtaining a priori estimates for (5.1). The convective term prevents us from a straightforward application of the arguments used in Section 4. The results derived in this section are at a far less satisfactory stage.

We start with a lemma analogous to Lemma 4.1.

LEMMA 5.1 ($W^1(L^1)$ A Priori Estimate) *Consider* (5.1) *subject to the initial condition* $u(x,t=0)=u_0(x)\in W^1(L^1)$ *and the homogeneous Neumann boundary condition* (4.3)*. Assume also that the convective flux* $f(u)$ *is convex and that its second derivative has an upper bound, that is,* $\forall u,\ 0\le f''(u)\le\beta$*. Then for* $t\le T$*, a classical solution satisfies*

$$\|u_x(\cdot,t)\|_{L^1}\le\|u_0'(\cdot)\|_{L^1}+(2+\beta t)(x_1-x_0)\,. \tag{5.2}$$

PROOF: Differentiating equation (5.1) with respect to x and denoting $w=u_x$, we obtain

$$w_t=\nu Q(w)_{xx}-(f'(u)w)_x\,. \tag{5.3}$$

Multiplying (5.3) by $\operatorname{sgn}(|w|-1)\operatorname{sgn}(w)$ followed by an integration over (x_0,x_1) yields

$$\begin{aligned}&\frac{d}{dt}\||w(\cdot,t)|-1\|_{L^1}\\ &\quad=\nu\int_{x_0}^{x_1}Q(w)_{xx}\operatorname{sgn}(|w|-1)\operatorname{sgn}(w)dx\\ &\qquad-\int_{x_0}^{x_1}(f'(u)w)_x\operatorname{sgn}(|w|-1)\operatorname{sgn}(w)dx=:\mathcal{I}_1+\mathcal{I}_2\,.\end{aligned} \tag{5.4}$$

As proved in Lemma 4.1, the first integral in the RHS of (5.4), $\mathcal{I}_1$, is non-positive. The second integral, $\mathcal{I}_2$, can be rewritten as

$$\mathcal{I}_2=-\sum_j\zeta(\sigma_j)f'(u)w\Big|_{x_{\sigma_j^l}}^{x_{\sigma_j^r}}, \tag{5.5}$$

where the $(\sigma_j,\zeta(\sigma_j))$ are the same as in (4.7). Without loss of generality, we consider $w(x,t)$ to behave qualitatively as in Figure 5.1. Other cases can be treated analogously.

For the present choice of $w(x)$,

$$\begin{aligned}\mathcal{I}_2\ =\ &-\Big\{[f'(u(b,t))-f'(u(a,t))]+[f'(u(d,t))-f'(u(c,t))]\\ &+\ [f'(u(d,t))-f'(u(a,t))]+[f'(u(b,t))-f'(u(c,t))]\Big\}\\ =:\ &\mathcal{I}_{21}+\mathcal{I}_{22}+\mathcal{I}_{23}+\mathcal{I}_{24}\,.\end{aligned} \tag{5.6}$$

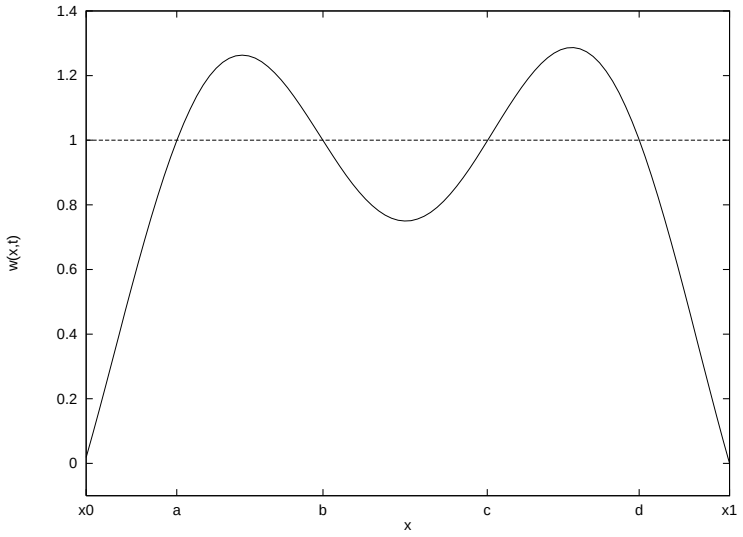

Figure 5.1. $w(x,t)$.

The first three terms in the RHS of (5.6), $\mathcal{I}_{21}$, $\mathcal{I}_{22}$, and $\mathcal{I}_{23}$, are negative due to the monotonicity of f' and the positivity of $w = u_x$. The last term in the RHS of (5.6), $\mathcal{I}_{24}$, is positive but can be bounded using the mean value theorem and the boundedness of f'',

$$\mathcal{I}_{24} = f''(\xi)u_x(\eta,t)(c-b) \le \beta(x_1 - x_0)\,. \tag{5.7}$$

Here we also made use of the boundedness of $w = u_x$ by 1 in $[b,c]$ (see Figure 5.1). Hence

$$\frac{d}{dt}\,||w|-1|_{L^1} \le \beta(x_1 - x_0)\,,$$

and the lemma follows. ∎

Lemma 5.1 leads to a weak maximum principle for the solutions of (5.1). Unlike Corollary 4.2, the bound obtained for the L^∞-norm of the solution now depends on time as well, and thus the L^∞-norm of the solution may increase linearly in time.

COROLLARY 5.2 (Maximum Principle) *Consider equation* (5.1) *subject to the initial condition* $u(x,t=0) = u_0(x) \in W^1(L^1)$ *and to the homogeneous Neumann boundary conditions* (4.3)*. Then for* $t \le T$*, a classical solution*

satisfies

$$\|u(\cdot,t)\|_{L^\infty} \le C_T\,. \tag{5.8}$$

Here the constant C_T depends on the initial datum u_0, on the time T, and on the size of the domain $(x_1 - x_0)$.

We do not know whether it is possible to obtain an L^∞-bound on u_x, but we are able to derive an Oleinik-type estimate [8] for equation (5.1) as follows:

LEMMA 5.3 (A One-Sided Estimate on u_x) *Consider equation* (5.1) *subject to the smooth initial condition $u(x,t=0) = u_0(x)$ and to the homogeneous Neumann boundary condition* (4.3)*. Assume that the convective flux is convex and that $\forall u$, $f''(u) \ge \alpha \ge 0$. Then for $t \le T$, its classical solution satisfies*

$$u_x(x,t) \le \max\left(\left(\alpha t + \frac{1}{\max_x [u_x(\cdot,0)]_+}\right)^{-1}, 1\right), \tag{5.9}$$

where $(\cdot)_+ := \max(\cdot, 0)$.

PROOF: Differentiating (5.1) with respect to x and denoting $w = u_x$, we obtain

$$w_t + f''(u)w^2 + f'(u)w_x = \frac{w^2-1}{(1+w^2)^2} w_{xx} + \left(\frac{w^2-1}{(1+w^2)^2}\right)_x w_x\,.$$

Denoting $y(t) := \max_x w(x,t)$, we deduce that either $y(t) < 1$ or $\dot{y} + \alpha y^2 \le 0$, and the lemma follows. ∎

Lemma 5.3 can also be extended to more general initial boundary conditions (see the remark following Lemma 4.6).

The embedded instability of equation (5.1) in the regions of small gradients presents a major challenge in implementing numerical algorithms for its solutions. The analytical results guided us to derive a numerical scheme that allows a linear growth in the L^∞ and the $W^1(L^1)$ norms of the solution. Figures 5.2 and 5.3 display the results of our numerical studies at two different times for the IBV problem:

$$\begin{cases} u_t + \frac{1}{2}(u^2)_x = -\left(\frac{u_x}{1+u_x^2}\right)_x\,, \quad x \in [-1, 15] \\ u_0(x) = \sin(x)\,, \quad u(-1,t) = \sin(-1)\,, \quad u(15,t) = \sin(15)\,. \end{cases} \tag{5.10}$$

We have used an adaptive Lax-Friedrichs-type numerical scheme. At each time level, the time step Δt was taken so as to satisfy the total variation limit (5.2).

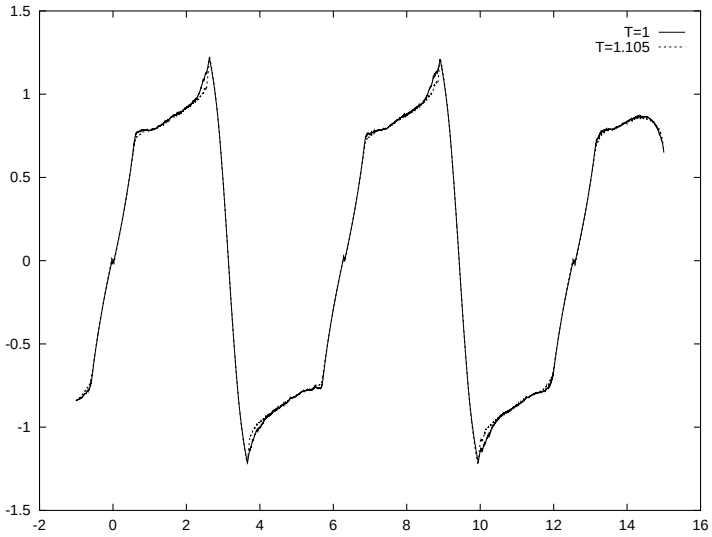

Figure 5.2. Problem (5.10).

In Figure 5.3 we consider in more detail two unstable domains of the solution shown in Figure 5.2. Although one is tempted to consider this pattern as the beginning of a fractal structure, we could not at this stage come to a definite conclusion regarding this phenomenon.

In conclusion, we would like to stress two problems related to these numerical results:

1. Can the available dissipation allow a formation of shocks? Lemma 5.3 provides an upper bound on the derivative u_x but not a lower bound.

2. Are the small staircase structures we observe in the unstable, small-gradients region typical of the dynamics of this problem or are they merely numerical artifacts?

Acknowledgment. This work was supported in part by a grant from the Israel Science Foundation. Part of the work of P. R. was carried out while visiting the Courant Institute and was supported by AFOSR Grant F49620-95-1-5065.

Bibliography

[1] Gilbarg, D., and Trudinger, N. S., *Elliptic Partial Differential Equations of Second Order*, 2nd ed., Springer-Verlag, Berlin, 1983.

[2] Goodman, J., Kurganov, A., and Rosenau, P., in preparation.

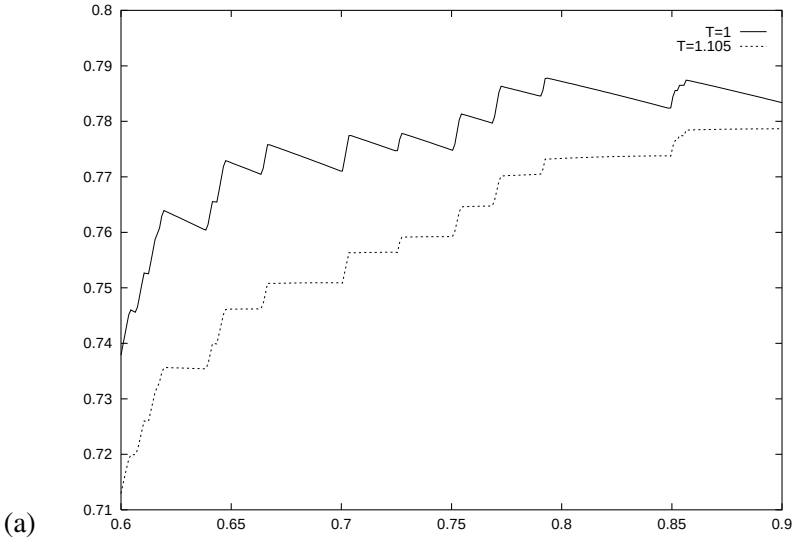

(a)

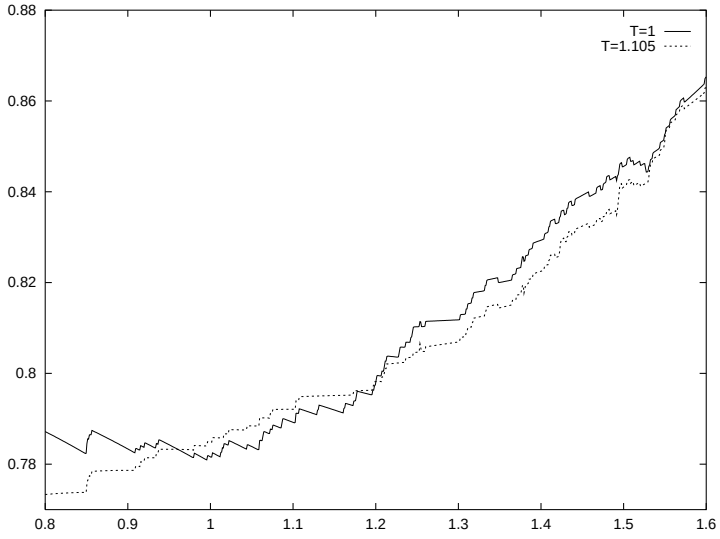

(b)

Figure 5.3. Problem (5.10). (a) Zoom on the $[0.6, 0.9]$ interval. (b) Zoom on the $[0.8, 1.6]$ interval.

[3] John, F., *Partial Differential Equations*, 4th ed., Springer-Verlag, New York, 1982.

[4] Kurganov, A., and Rosenau, P., *Effects of a saturating dissipation in Burgers-type equations*, Comm. Pure Appl. Math. 50(8), 1997, pp. 753–771.

[5] Ladyženskaja, O. A., Solonnikov, V. A., and Ural′ceva, N. N., *Linear and Quasilinear Equations of Parabolic Type*, Translations of Mathematical Monographs 23, American Mathematical Society, Providence, R.I., 1967.

[6] Lar′kin, N. A., Novikov, V. A., and Yanenko, N. N., *Nonlinear equations of varying type*, "Nauka" Sibirsk. Otdel., Novosibirsk, 1983. (in Russian).

[7] Nessyahu, H., and Tadmor, E., *Nonoscillatory central differencing for hyperbolic conservation laws*, J. Comput. Phys. 87(2), 1990, pp. 408–463.

[8] Oleinik, O. A., *Discontinuous solutions of non-linear differential equations*, Amer. Math. Soc. Transl. (2) 26, 1963, pp. 95–172.

[9] Perona, P., and Malik, J., *Scale-space and edge detection using anisotropic diffusion*, IEEE Trans. Pattern Anal. Machine Intell. 12, 1990, pp. 629–639.

[10] Rosenau, P., *Free energy functionals at the high-gradient limit*, Phys. Rev. A. 41, 1990, pp. 2227–2230.

[11] Schochet, S., private communication.

[12] Slemrod, M., *Dynamics of measured valued solutions to a backward-forward heat equation*, J. Dynamics Differential Equations 3(1), 1991, pp. 1–28.

[13] Tadmor, E., and Tassa, T., *On the homogenization of oscillatory solutions to nonlinear convection-diffusion equations*, Adv. Math. Sci. Appl. 7(1), 1997, pp. 93–117.

ALEXANDER KURGANOV
Department of Mathematics
Tel-Aviv University
Tel-Aviv 69978
ISRAEL
E-mail:
kurganov@math.tau.ac.il

DORON LEVY
Department of Mathematics
Tel-Aviv University
Tel-Aviv 69978
ISRAEL
E-mail:
dlevy@math.tau.ac.il

PHILIP ROSENAU
Department of Mathematics
Tel-Aviv University
Tel-Aviv 69978
ISRAEL
E-mail:
rosenau@math.tau.ac.il

Received June 1997.